MedCrave
Step into the World of Research
Aeronautics and Aerospace Open access Journal

Research Article
Open Access
CrossMark

Analysis of parameters considered for subsonic wind tunnel and supersonic wind tunnel design with suitability of material properties useful for blades design: A MATLAB simulation investigation

Abstract

Supersonic and subsonic wind tunnel and laminate material properties useful for blades design using MATLAB codes are investigated. In present investigation parameters such as mass flow rate vs throat area, test duration vs mass flow rate, area Mach number relation and test duration vs throat height are considered for supersonic wind tunnel design. Similarly parameters such as pressure test section, pressure distribution, diffuser section head losses, and hydraulic diameter at test section are considered for subsonic wind tunnel design. The variations of ratio size of the open to test section, variable length of tunnel, variable nozzle length, and variable test section area for determining the variable critical dimensions (throat area and expansion ratio), estimating the attainable test duration, volumetric flow rate, mass flow rate, energy ratio for design of a supersonic nozzle and diffuser to minimize shocks in the test section. For the choice of blade material design; three different types of material properties are studied. The effects of ply angle on sensitivity of laminate material properties: cases of young modulus stiffness, Poisson ratio stiffness and shear modulus stiffness properties of a laminate for various orientations the ply angles between (0^0 and 90^0) in bending is considered. Comparing three types material properties, material Ref [**33**] found to have higher Young modulus stiffness in longitudinal direction, Shear modulus stiffness and Poisson ratio stiffness parameters for ply angles (15^0,30^0,45^0,60^0,75^0 and 90^0) except Young modulus stiffness in lateral direction considered for the choice of blade design material.

Keywords: airfoil, angle of attack, lift coefficient, drag coefficient, gliding ratio, lift force, young modulus, poisson ratio, micromechanical, stiffness properties, graphite epoxy, stochastic optimisation.

Volume 9 Issue 4 - 2025

Rajesh Kumar
Delhi Technological University, New Delhi-100042, India

Correspondence: Rajesh Kumar, Department of Mechanical Engineering, Delhi Technological University, New Delhi-100042, India, Tel +919953116357

Received: November 26, 2025 | **Published:** December 26, 2025

Introduction

Earlier researchers made significant contribution in this direction McCabe A.,[1] studied the design of a supersonic nozzle. Barlow, Pope and Rae.,[2–4] investigated the low and high speed wind tunnel testing. Delery and Marvin.,[5] investigated the shock-save boundary layer interaction. Sankar.,[6] studied the parts of wind tunnel and Giancoli and Douglas.,[7] gave concepts of physics for scientists and engineers with modern physics. Anderson.,[8] studied the supersonic flight and the breaking of the sound barrier. Anderson.,[9] highlighted the modern compressible flow with historical perspective discussing the sequential progress in fluid flow. Kotwani.,[10] investigated the wind tunnel performance analysis. Baals and Corliss.,[11] investigated the wind tunnels of NASA to further explore universe missions. John et al.,[12] presented the concept of Gas dynamics. Henry et al.,[13] contributed for orders of magnitude. Carlone.,1[4] explained about the building a wind tunnel. Nott et al.,[15] studied the supersonic, variable-throat, blow down wind tunnel control using genetic algorithms, neural networks, and gain scheduled PID. Lu et al.,[16] investigated the rapid valve opening technique for supersonic blow down tunnel. Baals.,[17] studied the whirling arms and the first wind tunnels. Aerolab, New York.,[18] studied the modern compressible flow. The low-speed wind tunnel testing concept was given in.[19] Wind Tunnel Corporation studied about vertical wind.

Ample research is also available on composite material characterisation. Some of noted are as Barlow et al.,[20] studied the low-speed Wind Tunnel testing. Williams.,[21] studied for nonlinear mechanical and actuation characterization of Piezoceramic fiber composites. Kudva.,[22] worked on smart wing project. Vos et al.,[23] investigated the morphing wing flight control via postbuckled precompressed piezoelectric actuators. Bilgen.,[24] studied the macro fiber composite actuated unmanned air vehicles: design, development and testing. Development and flight testing of a morphing aircraft is studied by.[25] Stewart et al.,[26] investigated the design of the air force research laboratory micro aerial vehicle research conjurations. Barbero.,[27] studied the finite element analysis of composite materials. Light weight high voltage electronic circuits; for piezoelectric composite actuators investigated by Bilgen et al.,[28] Bilgen.,[29] studied the aerodynamic and electromechanical design, modeling, and implementation of Piezo-composite airfoils. Smart Material Corporation publication investigated.[30] Shen.,[31] investigated the hydrothermal effects on the post buckling of shear deformable laminated plates. Ramesh Pandey et al.,[32] studied the hydrothermal elastic post buckling response of laminated composite plates. Aydin et al.,[33] investigated the comparison of stochastic search optimization algorithms for the laminated composites under mechanical and hydrothermal determination of the effects of ply angle on sensitivity of laminate material properties.

Analysis of parameters considered for subsonic wind tunnel and supersonic wind tunnel design with suitability of material properties useful for blades design. A MATLAB simulation investigation is not studied so far to the best of author's knowledge.

Materials and methodology

In first part subsonic wind tunnel design parameters for pressure test section, pressure distribution, diffuser section, head losses, hydraulic diameter at test section and for subsonic wind tunnel design parameters mass flow rate vs throat area, test duration vs mass flow rate, area much number relation, test duration vs throat height are taken for study. MATLAB codes are used for analysis.

In present investigation parameters such as mass flow rate vs throat area, test duration vs mass flow rate, area Mach number relation and test duration vs throat height are considered for supersonic wind tunnel design. Similarly parameters such as pressure test section, pressure distribution, diffuser section head losses, and hydraulic diameter at test section are considered for subsonic wind tunnel design.

In second part of investigation for blade design material properties, three types of materials of graphite epoxy materials are chosen as mentioned in ref.,[31–33] written as material 1, material 2 and material 3 respectively. MATLAB codes are used for analysis to find out suitability for blade design.

When looking at the pressure throughout the tunnel, the main focus is changes between the reservoir section and the test section, test section and the diffusion section. The following analysis consists of the pressure changes in the test section as the velocity of the air in the tunnel increases to the max speed. This analysis was done to ensure that the amount of pressure that will be built up at maximum velocity is feasible. The analysis started with Bernoulli's equation for ideal flow.

$p_1 + 1/2\ \rho V_1^2 = p_2 + 1/2\ \rho V_2^2$ (1)

The geometrical and non-mechanical properties considered are: a=b=235mm, t= 6mm, Thermal coefficient α_1=-0.3 * 10-6, $\alpha_{\beta 2}$ =28.1 * 10-6, Moisture coefficient α_1=0, α_2=0.44.

Parameters considered for subsonic wind tunnel design

Pressure test section

Maximum Velocity (C_{max}) = 0:1:255 m/s.

Density of air (rho) = 1.225 Kg/m^3

Initial pressure (p_1) = 1 ata,

Area Ratio (Open to teat section) =6

a_2=24.

Test section area $a_2 = a_2$ * (0.3048) ^ 2 in meters. $p_1 = p_1$ * 101.31* 1000 N/m^2

$C_1 = (a_2 * C_{max})$ / a1 Initial Velocity.

$p_2 = p_1 + (rho/2) * (C_{max})$ ^ 2-C1 ^ 2. (2)

$p_2 = (p_2 / 1000)$ / 101.31 ata. (3)

Pressure distribution

Maximum Velocity = 255 m/s.

Density (rho) =1.225 Kg/m^3.

Initial pressure (p1) = 1 ata

Area Ratio (Open to teat section) =6.

a_2=24.

Test section area $a_2 = a_2$*(0.3048) ^2 in meters

$p_1 = p_1$ * 101.31 * 1000 N/m^2. (4)

Area of open system (a1) = (a_2*Area Ratio-0.02:9.2)

$C_1 = (a_2 * C_{max}) / a_1$ Initial Velocity.

$p_2 = p_1 + (rho/2) * (C_1)$ ^ 2 - Cmax^2 (5)

Diffuser section

Exit area $a_3 = (a_2:0.02:a_2$ * Area Ratio),

Exit Velocity $C_3 = (a_2/a_3)\ C_{max}$

Exit Pressure p_3 = p-(rho/2) * (Cmax ^ 2 * p2) - C_3 ^ 2. (6)

p = (p/1000) / 101.3.

$p_2 = (p_2/1000)$ / 101.31 ata.

$p_3 = (p_3/1000)$ / 101.31 ata.

Head losses

Head losses

Density of air (rho) = 1.225 Kg/m^3,

Area Ratio (Open to teat section) = 6, a_2 = 24

$a_2 = a_2$ * (0.3048) ^ 2 in meters,

Maximum Free Velocity m/s = (5:5:251)

Flow q = 0.5 * rho * (Free Velocity) ^2,

Specific heat ratio = 1.4, Viscosity = 1.783 * 10 ^ -5

Total Pressure drop H_1 = 1,

Local section Loss K_1 = H1 / q, Test Area = a_2

Local Area = sqrt (Area test) ^ 2 * q / q_{test})

Hydraulic diameter at test section

D (h) = a_1 * sqrt (area test/pi),

Length of Test Section = 3

Vertically Test Section Diameter Dt = Dh,

Test Mach number = 0.7

Reynolds Number = Re,

For z = (1:1:4), f = F

K Test = f*(Test / Dh),

Ar = a_1 / a_2,

L = 120 * (0.3048) ^2

Diameter at 1-1 section = 16.97*(0.3048) ^ 2

Theta = a tan (0.5*sqrt (Ar) - 1 / (L/D1)

Theta = Theta * (180/pi), Flow Rate (Q)

Q(x) = (6*(0.3048) ^ 2*4*0.3048 ^ 2*V

Parameters considered for supersonic wind tunnel design

Mass flow rate vs throat area

Stagnation Temperature T0 = 293K,

Stagnation Pressure P0 = 101325 Pa

Citation: Kumar R. Analysis of parameters considered for subsonic wind tunnel and supersonic wind tunnel design with suitability of material properties useful for blades design:A MATLAB simulation investigation. *Aeron Aero Open Access J.* 2025;9(2):106–116. DOI: 10.15406/aaoaj.2025.09.00241

R = 287, Cross Section Area at Throat (A) = (1:0.2:9) cm^2

Mass Flow Rate at Throat = Pressure* Area

Test duration vs mass flow rate

Pressure in Vacuum Chamber pe = 53499.6 pa,

Stagnation Temperature Tt = 293K

Volume of Vacuum Chamber = 2.317 m^3, R=287

Test Duration t = (V*pe/Mass flow rate in throat*R*Tt) * (1-pi/pe)

Initial Pressure in Vacuum Chamber pi= 6.68745 pa,

Mass flow rate = (0:0.001:0.04) Kg/s

Area Mach number relation

Specific heat ratio = 1.4,

Range of Mach number M = (1:0.2:5)

Area Ratio (A / A*) = sqrt (1/m^2) *(2/(r+1) * (2/r+1) * 1+(r+1) * m^2/2) ^ (r+1/r-1)

Test duration vs throat height

Specific heat ratio = 1.4,

Stagnation Pressure Pt = 101325 pa

R = 287, Width of Throat w = 3.81 cm

Initial pressure of pump down Vacuum Chamber pi = 6.6875

Pressure in Vacuum chamber at the end of run pe = 53499.6

Volume of vacuum Chamber v = 2.317m^3,

Height of throat h = (0.1:0.1:2)

Graphite-epoxy material (1) Ref.,[31]

E_1 = 1.38e + 11.E_2=9 .70e+09.G_{12} = 2.67e + 09 v_{12} = 0.2578. G_{13} = 2.679e + 09. G_{23} = 1.339e + 09.

Graphite-epoxy material (2) Ref.,[32]

E_1 = 2.5e + 10,

E_2 = 1.0e + 09,

G_{12} = 500000000,

v_{12} = 0.25,

G_{13} = 500000000,

G_{23} = 200000000

Graphite-epoxy material (3) Ref.,[33]

E_1 = 2.77e + 11,

E_2 = 7.05e + 09,

G_{12} = 3.488e + 09,

v_{12} = 0.285,

G_{13} = G_{12},

G_{23} = 0.5 * G_{12}

(Figure 1)

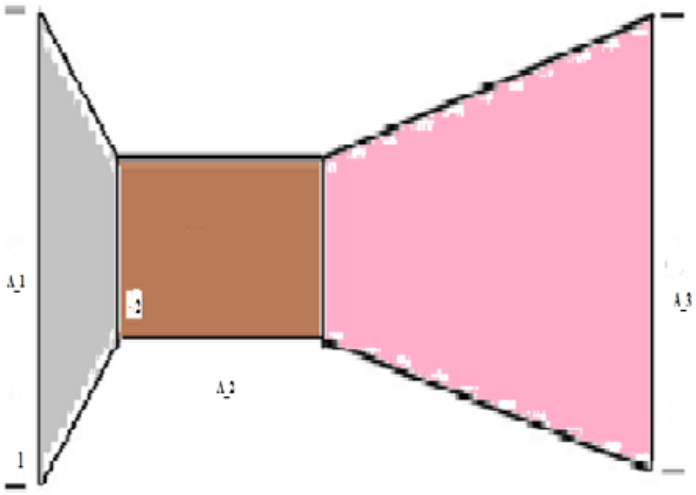

Figure 1 Geometry of Wind Tunnel for test.

Figure 2 in this test section the ratio size of the open to test section= 6, length of tunnel = 120 m, nozzle length - meters =6 and test section area 24 m^2 stagnation temperature of ambient air is taken 293 K The study is carried out for test section, Nozzle, diffuser and constant area. Total pressure drop for different flow rate is studied.

Citation: Kumar R. Analysis of parameters considered for subsonic wind tunnel and supersonic wind tunnel design with suitability of material properties useful for blades design:A MATLAB simulation investigation. *Aeron Aero Open Access J.* 2025;9(2):106–116. DOI: 10.15406/aaoaj.2025.09.00241

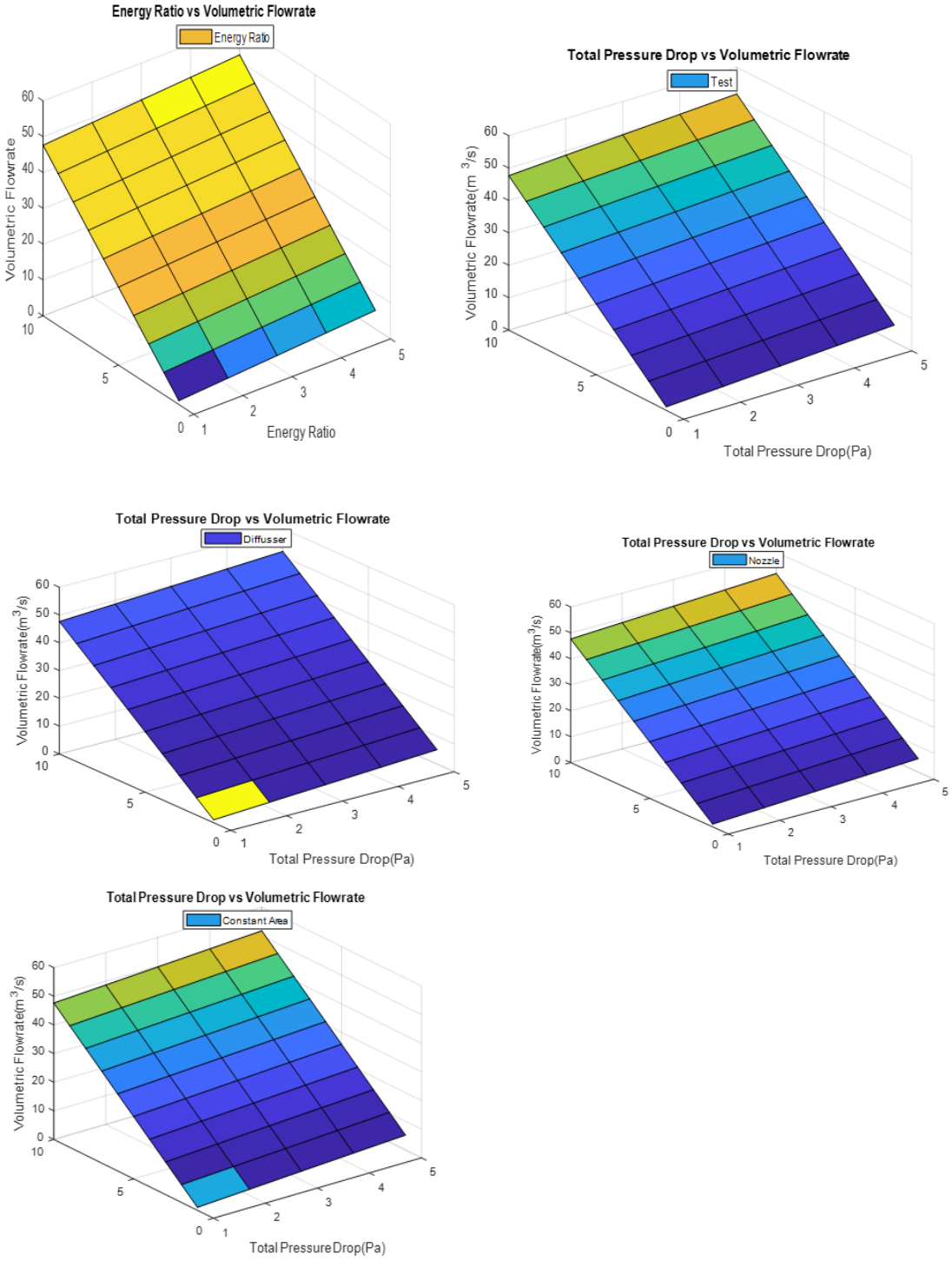

Figure 2 The ratio size of the open to test section= 6, length of tunnel = 120 m, nozzle length - meters =6 and test section area 24 m^2 stagnation temperature of ambient air is taken 293 K.

Figure 3 in this test section the ratio size of the open to test section= 2-10, length of tunnel = 120 m, nozzle length - meters =6 and test section area = 24 m^2 stagnation temperature of ambient air is taken 293 K. The study is carried out for test section, Nozzle, diffuser and constant area. Total pressure drop for different flow rate is studied.

Citation: Kumar R. Analysis of parameters considered for subsonic wind tunnel and supersonic wind tunnel design with suitability of material properties useful for blades design: A MATLAB simulation investigation. *Aeron Aero Open Access J.* 2025;9(2):106–116. DOI: 10.15406/aaoaj.2025.09.00241

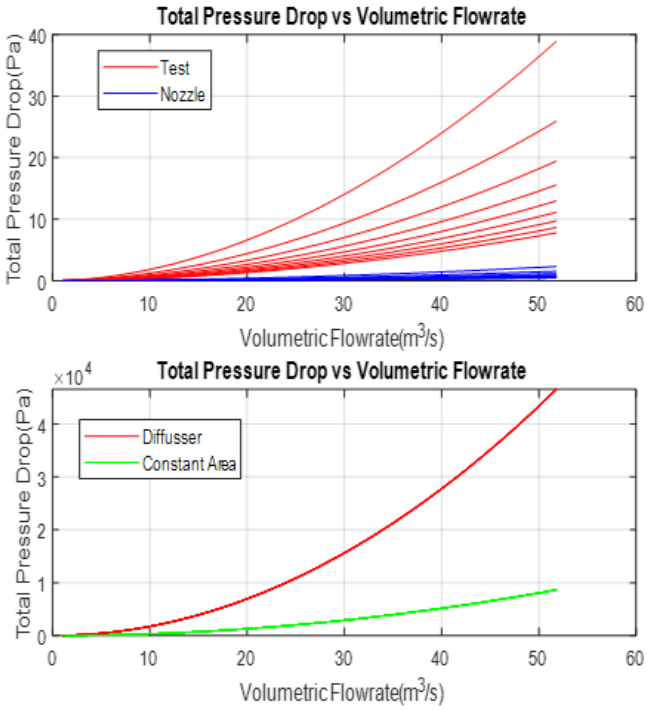

Figure 3 The ratio size of the open to test section= 2-10, length of tunnel = 120 m, nozzle length - meters =6 and test section area = 24 m^2 stagnation temperature of ambient air is taken 293 K.

It can be noticed that for different volumetric air flow rates varying (0 to 50) the total pressure drop behaves differently for Test section and Nozzle. For test section the drop of total pressure is higher compared to Nozzle section. Similarly, total pressure drop for diffuser is much higher compared to constant area of wind tunnel and the ratio size of the open to test section does not contribute as in case of test section.

Another graph represents the energy ratio vs. volumetric flow rate. Here we can see that for flow rate (0 to 10), there is sharp rise in energy ratio (energy without losses and energy with losses considerations) and after that increases slowly. Here losses are less significant.

Figure 4 Mass flow rate as a function of throat area is studied in figure4. Stagnation temperature of ambient air varied from 283 to 303K. Cross sectional area of throat A cm^2 is varied from 1 to 9, Po = 101325 in Pascal's is the stagnation pressure of ambient air. Here we see that air mass flow rate significantly increases on increase of throat cross sectional area and also varies on varying stagnation temperature.

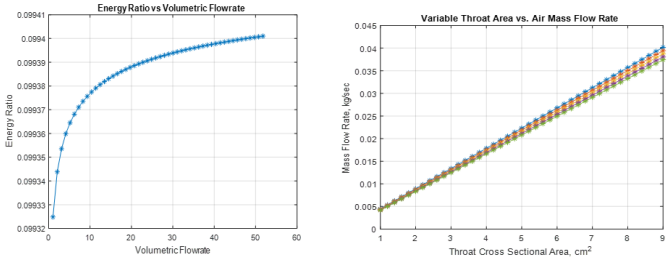

Figure 4 Mass flow rate as a function of throat area is studied

Figure 5 In this test section the ratio size of the open to test section= 6, length of tunnel = 120 m, nozzle length - meters =6 and test section area varied from 20 to 28 m^2, stagnation temperature of ambient air is taken 293 K. The study is carried out for test section, Nozzle, diffuser and constant area. Total pressure drop for different flow rate is studied.

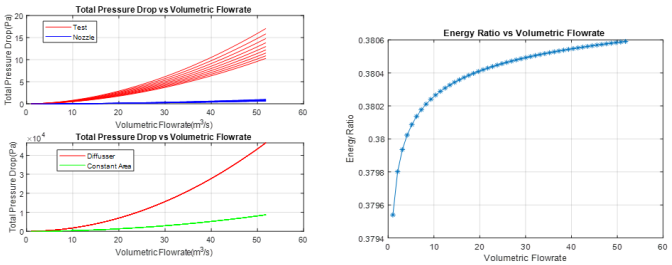

Figure 5 The ratio size of the open to test section= 6, length of tunnel = 120 m, nozzle length - meters =6 and test section area varied from 20 to 28 m^2, stagnation temperature of ambient air is taken 293 K.

It can be noticed that for different volumetric air flow rates varying (0 to 50), the total pressure drop behaves differently for Test section and Nozzle. For test section the drop of total pressure is significant and even drop between 10 and above compared to Nozzle section. Similarly, total pressure drop for diffuser is much higher compared to constant area of wind tunnel and the ratio size of the open to test section does not contribute as in case of test section. Another graph represents the energy ratio vs. volumetric flow rate. Here we can see that for flow (0 to 10), there is sharp rise in energy ratio (energy without losses and energy with losses considerations) and after that increases slowly. Here losses are more significant. Energy ratio is much higher for test section area varied.

Figure 6 Stagnation temperature of ambient air is varied from 283 to 303 K. Initial pressure of pumped-down vacuum chamber is Pi=6.68745 Pascal mass flow rate is taken as (0 to 0.04) kg/sec. From figure it is clearly seen that for small amount of air mass flow rate there is need of higher test duration and then sharp decline occur when the mass flow rate increases and a minimum value reaches. On varying stagnation temperature of ambient air there is slight variations in test duration curve.

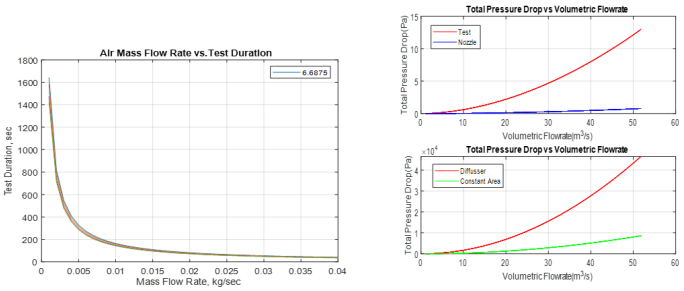

Figure 6 Stagnation temperature of ambient air is varied from 283 to 303 K. Initial pressure of pumped-down vacuum chamber is Pi=6.68745 Pascal mass flow rate is taken as (0 to 0.04) kg/sec.

Figure 7 In this test section the ratio size of the open to test section= 6, length of tunnel is varied from100 to 130 m, nozzle length - meters =6 and test section area taken is 24 m^2, stagnation temperature of ambient air is taken 293 K The study is carried out for test section, Nozzle, diffuser and constant area. Total pressure drop for different flow rate is studied. It can be noticed that for different volumetric air flow rates varying (0 to 50), the total pressure drop behaves differently for Test section and Nozzle. For test section the drop of total pressure is significant compared to Nozzle section. Similarly, total pressure drop for diffuse is much higher compared to constant area of wind tunnel and the ratio size of the open to test section does not contribute as in case of test section. Another graph represents the energy ratio

Citation: Kumar R. Analysis of parameters considered for subsonic wind tunnel and supersonic wind tunnel design with suitability of material properties useful for blades design:A MATLAB simulation investigation. *Aeron Aero Open Access J.* 2025;9(2):106–116. DOI: 10.15406/aaoaj.2025.09.00241

vs. volumetric flow rate. Here we can see that for flow 0 to 10, there is sharp rise in energy ratio (energy without losses and energy with losses considerations) and after that increases slowly. Here losses are more significant. Energy ratio is further higher test section area varied.

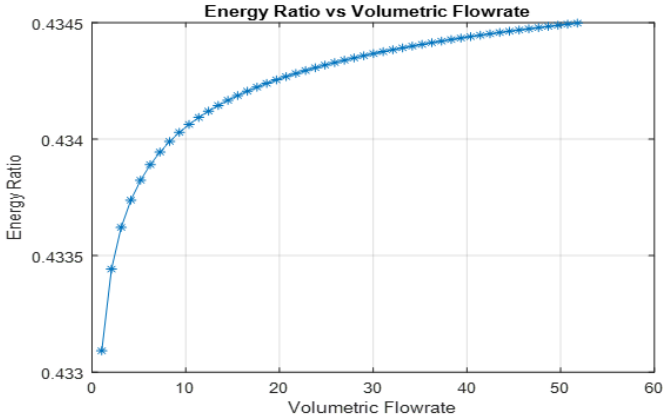

Figure 7 Test section the ratio size of the open to test section= 6, length of tunnel is varied from100 to 130 m, nozzle length - meters =6 and test section area taken is 24 m^2, stagnation temperature of ambient air is taken 293 K.

Figure 8 Stagnation temperature of ambient air is 293 K. Range of mach numbers is taken from (1 to 5).Variation of area ratios and its effects on Mach number is studied. It can be seen from the figure that up to area ratio 5 there is sharp rise in Mach number and then increases at slight slowly for maximum area ratio M25 and the Mach number reaches to 5.

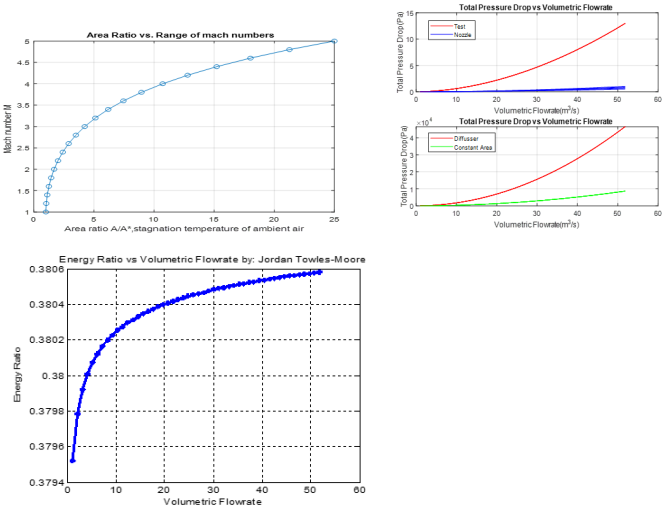

Figure 8 Stagnation temperature of ambient air is 293 K. Range of mach numbers is taken from (1 to 5).Variation of area ratios and its effects on Mach number.

Figure 9 In this test section the ratio size of the open to test section= 6, length of tunnel is 120 m, nozzle length - meters =4-6 and test section area taken is 24 m^2. Stagnation temperature of ambient air is taken 293 K the study is carried out for test section, Nozzle, diffuser and constant area. Total pressure drop for different flow rate is studied. It can be noticed that for different volumetric air flow rates varying 0 to 50 the total pressure drop behaves differently for Test section and Nozzle. For test section the drop of total pressure is significant compared to Nozzle section. Similarly, total pressure drop for diffuse is much higher compared to constant area of wind tunnel and the ratio size of the open to test section does not contribute as in case of test section. Another graph represents the energy ratio vs. volumetric flow rate. Here we can see that for flow (0 to 10), there is sharp rise in energy ratio (energy without losses and energy with losses considerations) and after that increases slowly. Here losses are more significant. Energy ratio is further higher test section area varied.

Figure 9 Test section the ratio size of the open to test section= 6, length of

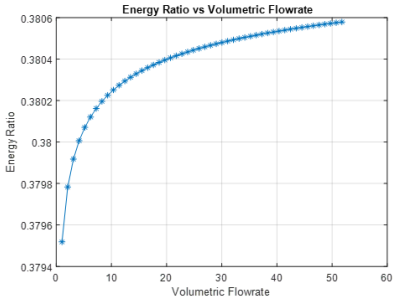

tunnel is 120 m, nozzle length - meters =4-6 and test section area taken is 24 m^2. Stagnation temperature of ambient air is taken 293 K

Figure 10 Stagnation temperature of ambient air is 293 K. Range of throat height is taken from (0 to 2).Variation of throat area and test duration is studied. It can be seen from the figure that up to throat area 0.4 there is sharp decline in test duration and then decreases at slight slowly for maximum throat height 2.

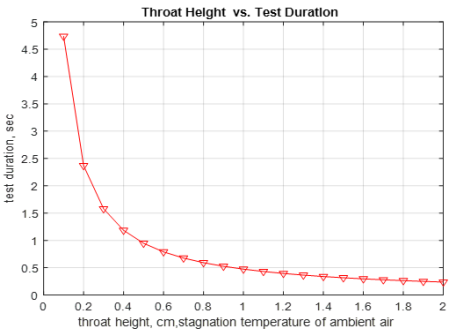

Figure 10 Stagnation temperature of ambient air is 293 K. Range of throat height is taken from (0 to 2).Variation of throat area and test duration.

Figure 11 Three types of material properties are analysed for the effects of ply angle 15^0 on variation of young modulus stiffness (Ex^b). It is seen that for material 3 properties has higher stiffness magnitude of 280 Gpa where as it is 140 Gpa for material1 properties and has lower value 25 Gpa for material2 at 0^0ply angle and decreases for all materials as ply angle increases.

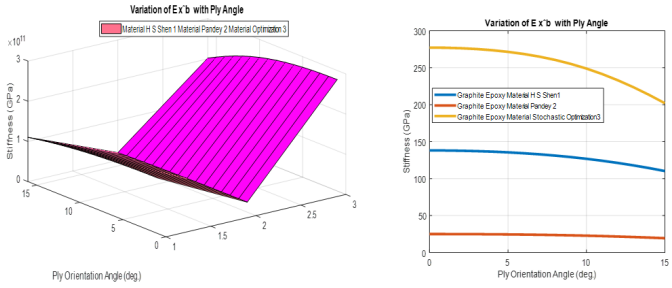

Figure 11 Three types of material properties are analysed for the effects of ply angle 15^0 on variation of young modulus stiffness (Ex^b).

Figure 12 Three types of material properties are analysed for the effects of ply angle 15^0on variation of young modulus stiffness

Citation: Kumar R.Analysis of parameters considered for subsonic wind tunnel and supersonic wind tunnel design with suitability of material properties useful for blades design:A MATLAB simulation investigation. *Aeron Aero Open Access J.* 2025;9(2):106–116. DOI: 10.15406/aaoaj.2025.09.00241

(Ey^b). It is seen that for material1 properties has higher stiffness magnitude of 9.8 Gpa where as it is 7.01 Gpa for material 3 properties and has lower value 1 Gpa for material2 at 0^0ply angle and decreases for material1 as ply angle increases.

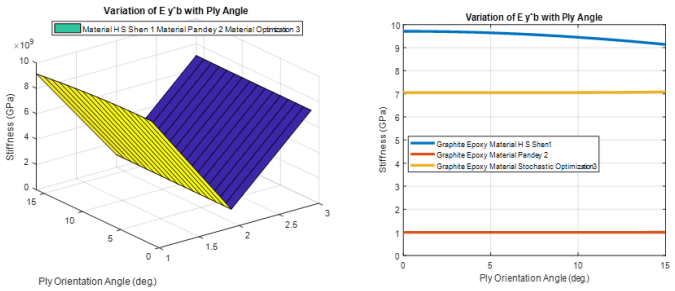

Figure 12 Three types of material properties are analysed for the effects of ply angle 15^0on variation of young modulus stiffness (Ey^b).

Figure 13 Three types of material properties are analysed for the effects of ply angle 15^0on variation of shear modulus stiffness (Gxy^b). It is seen that for material3 properties has higher stiffness magnitude of 4.0 Gpa where as it is 3.0 Gpa for material1 properties and has lower value 0.2 Gpa for material2 at 0^0ply angle and increases for all materials as ply angle increases.

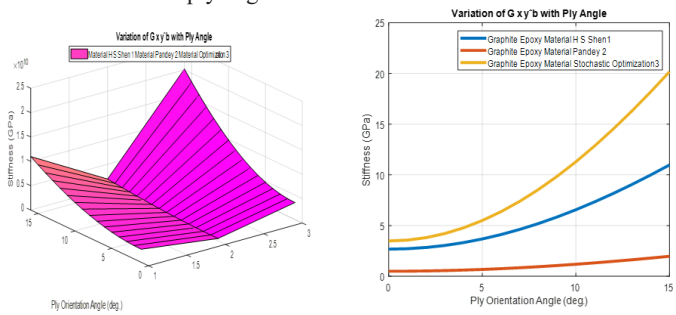

Figure 13 Three types of material properties are analysed for the effects of ply angle 15^0on variation of shear modulus stiffness (Gxy^b).

Figure 14 Three types of material properties are analysed for the effects of ply angle 15^0on variation of Poisson ratio stiffness (vxy^b). It is seen that for material 3 properties has higher stiffness magnitude of 0.25 GPa where as it is 0.2 GPa for material1 properties and has same value 0.2 GPa for material 2 at 0^0ply angle and increases drastically for material 3 and material 2 and lower for material 1 as ply angle increases.

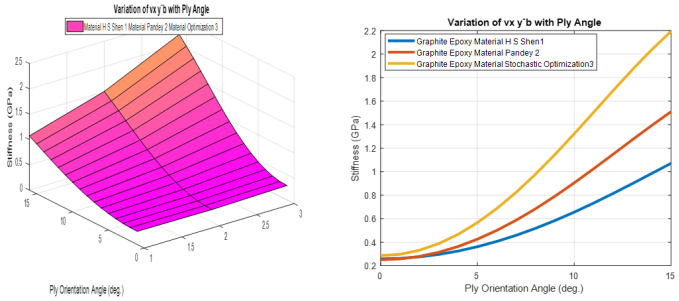

Figure 14 Three types of material properties are analysed for the effects of ply angle 15^0on variation of Poisson ratio stiffness (vxy^b).

Figure 15 Three types of material properties are analysed for the effects of ply angle 30^0on variation of young modulus stiffness (Ex^b). It is seen that for material 3 properties has higher stiffness magnitude of 275 GPa where as it is 145 GPa for material 1 properties and has lower value 25 GPa for material 2 at 0^0ply angle and decreases for all materials as ply angle increases.

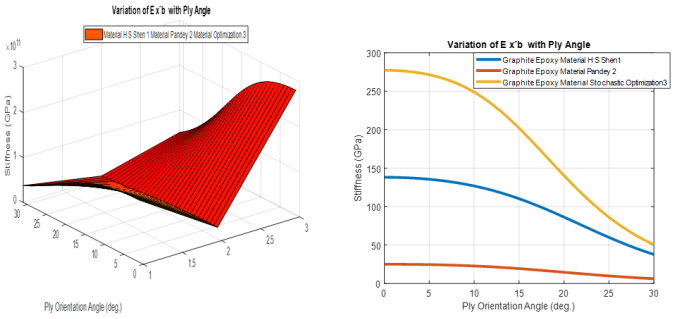

Figure 15 Three types of material properties are analysed for the effects of ply angle 30^0on variation of young modulus stiffness (Ex^b).

Figure 16 Three types of material properties are analysed for the effects of ply angle 30^0on variation of young modulus stiffness (Ey^b). It is seen that for material 1 properties has higher stiffness magnitude of 9.8 GPa where as it is 7.0 GPa for material 3 properties and has lower value 1.0 GPa for material 2 at 0^0ply angle and increases for all materials except material.1 as ply angle increases.

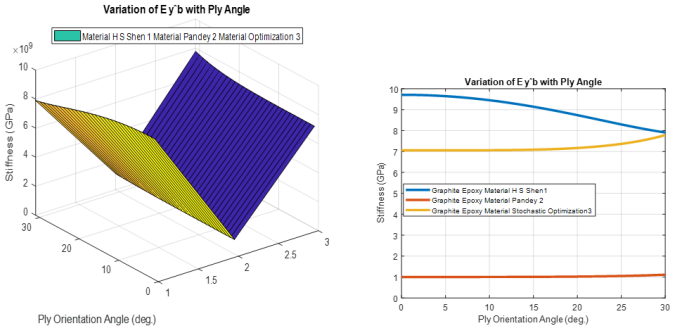

Figure 16 Three types of material properties are analysed for the effects of ply angle 30^0on variation of young modulus stiffness (Ey^b).

Figure 17 Three types of material properties are analysed for the effects of ply angle 30^0on variation of shear modulus stiffness (Gxy^b). It is seen that for material 3 properties has higher stiffness magnitude of 4.0 GPa where as it is 3.0 GPa for material 1 properties and has lower value 0.1 GPa for material 2 at 0^0ply angle and increases for all materials as ply angle increases.

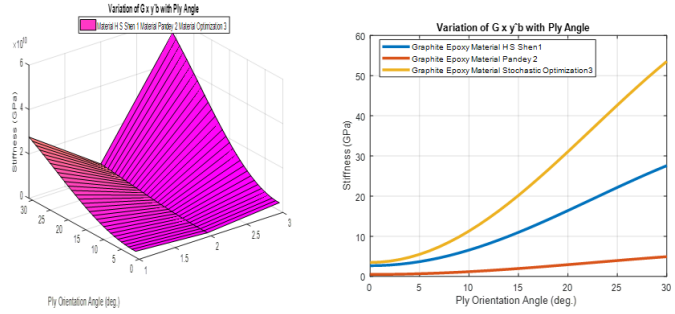

Figure 17 Three types of material properties are analysed for the effects of ply angle 30^0on variation of shear modulus stiffness (Gxy^b).

Figure 18 Three types of material properties are analysed for the effects of ply angle 30^0on variation of Poisson ratio stiffness (vxy^b). It is seen that for all material properties has same stiffness magnitude of 2.5 GPa at 0^0ply angle and increases and decreases for all materials as ply angle increases.

Citation: Kumar R. Analysis of parameters considered for subsonic wind tunnel and supersonic wind tunnel design with suitability of material properties useful for blades design:A MATLAB simulation investigation. *Aeron Aero Open Access J.* 2025;9(2):106–116. DOI: 10.15406/aaoaj.2025.09.00241

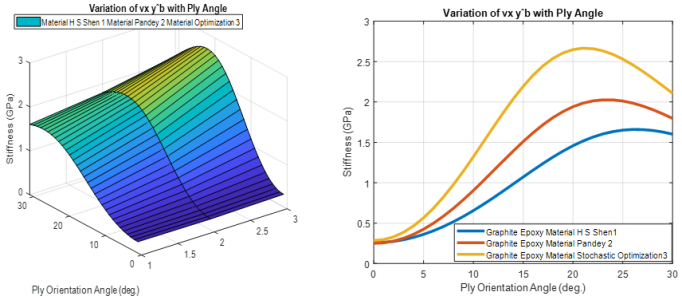

Figure 18 Three types of material properties are analysed for the effects of ply angle 30^{0}on variation of Poisson ratio stiffness (vxy^b).

Figure 19 Three types of material properties are analysed for the effects of ply angle 45^{0}on variation of young modulus stiffness (Ex^b). It is seen that for material 3 properties has higher stiffness magnitude of 275 Gpa where as it is 140 Gpa for material1 properties and has lower value 25 Gpa for material 2 at 0^{0}ply angle and decreases drastically for all materials as ply angle increases.

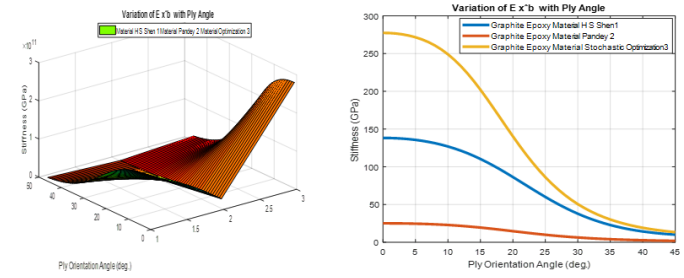

Figure 19 Three types of material properties are analysed for the effects of ply angle 45^{0}on variation of young modulus stiffness (Ex^b).

Figure 20 Three types of material properties are analysed for the effects of ply angle 45^{0}on variation of young modulus stiffness (Ey^b). It is seen that for material1 properties has higher stiffness magnitude of 9.8 Gpa where as it is 7.01 Gpa for material 3 properties and has lower value 1 Gpa for material 2 at 0^{0}ply angle and decreases and increase for material 1 and increases for material 2 and material 3 as ply angle increases.

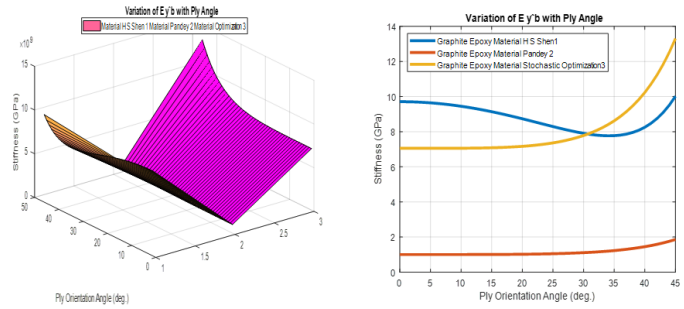

Figure 20 Three types of material properties are analysed for the effects of ply angle 45^{0}on variation of young modulus stiffness (Ey^b).

Figure 21 Three types of material properties are analysed for the effects of ply angle 45^{0}on variation of shear modulus stiffness (Gxy^b). It is seen that for material 3 properties has higher stiffness magnitude of 3.0 GPa where as it is 2.0 GPa for material 1 properties and has lower value 0.1 GPa for material 2 at 0^{0}ply angle and increases for all materials as ply angle increases.

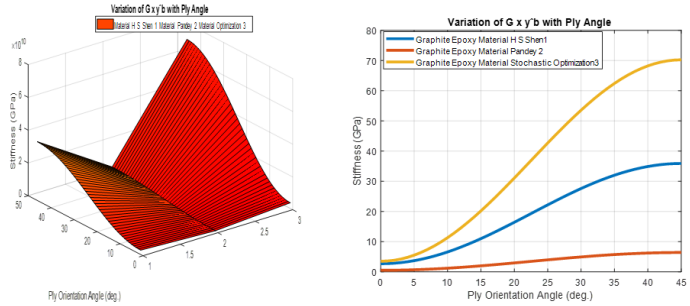

Figure 21 Three types of material properties are analysed for the effects of ply angle 45^{0}on variation of shear modulus stiffness (Gxy^b).

Figure 22 Three types of material properties are analysed for the effects of ply angle 45^{0}on variation of Poisson ratio stiffness (vxy^b). It is seen that for all material properties has same stiffness magnitude of 2.5 GPa at 0^{0}ply angle and increases and decreases for all materials as ply angle increases.

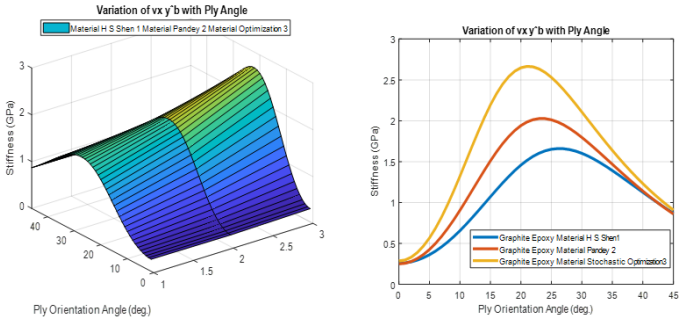

Figure 22 Three types of material properties are analysed for the effects of ply angle 45^{0}on variation of Poisson ratio stiffness (vxy^b).

Figure 23 Three types of material properties are analysed for the effects of ply angle 60^{0}on variation of young modulus stiffness (Ex^b). It is seen that for material 3 properties has higher stiffness magnitude of 275 Gpa where as it is 140 Gpa for material1 properties and has lower value 25 Gpa for material 2 at 0^{0}ply angle and decreases drastically to almost zero for all materials as ply angle increases.

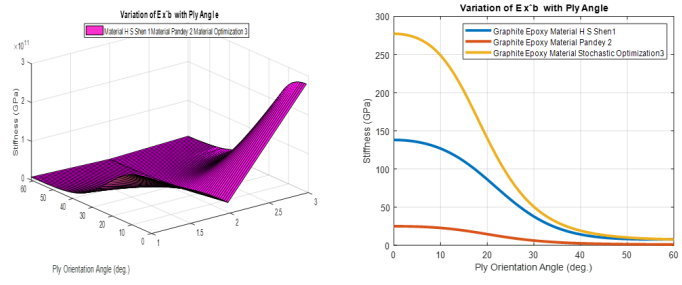

Figure 23 Three types of material properties are analysed for the effects of ply angle 60^{0}on variation of young modulus stiffness (Ex^b).

Figure 24 Three types of material properties are analysed for the effects of ply angle 60^{0}on variation of young modulus stiffness (Ey^b). It is seen that for material 1 properties has higher stiffness magnitude of 10 Gpa where as it is 8.0 Gpa for material 3 properties and has lower value 0.5 Gpa for material 2 at 0^{0}ply angle and decreases and increase for material 1 and increases for material 2 and material 3 as ply angle increases.

Citation: Kumar R. Analysis of parameters considered for subsonic wind tunnel and supersonic wind tunnel design with suitability of material properties useful for blades design:A MATLAB simulation investigation. *Aeron Aero Open Access J.* 2025;9(2):106–116. DOI: 10.15406/aaoaj.2025.09.00241

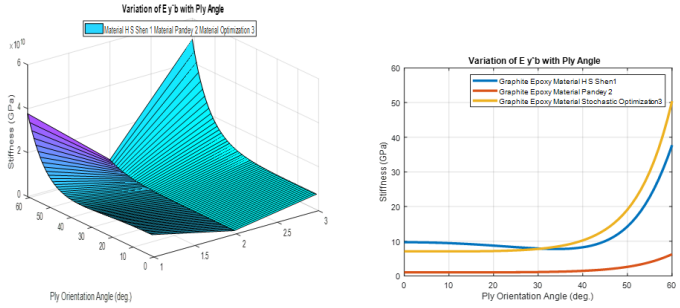

Figure 24 Three types of material properties are analysed for the effects of ply angle 60^{0}on variation of young modulus stiffness (Ey^b).

Figure 25 Three types of material properties are analysed for the effects of ply angle 60^{0}on variation of shear modulus stiffness (Gxy^b). It is seen that for material 3 properties has higher stiffness magnitude of 3.0 GPa where as it is 2.0 GPa for material 1 properties and has lower value 0.1 GPa for material 2 at 0^{0}ply angle and increases and decreases for all materials as ply angle increases.

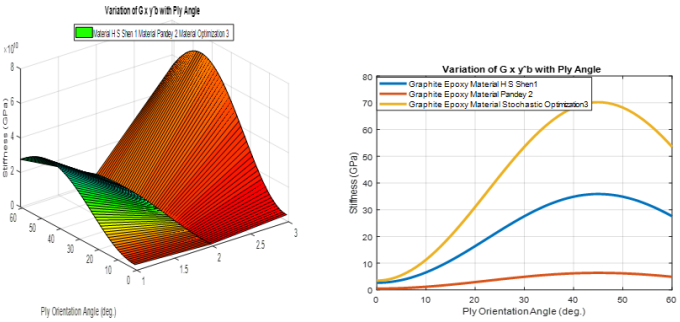

Figure 25 Three types of material properties are analysed for the effects of ply angle 60^{0}on variation of shear modulus stiffness (Gxy^b).

Figure 26 Three types of material properties are analysed for the effects of ply angle 60^{0}on variation of Poisson ratio stiffness (vxy^b). It is seen that for all material properties has same stiffness magnitude of 2.5 GPa at 0^{0}ply angle and increases and decreases for all materials as ply angle increases.

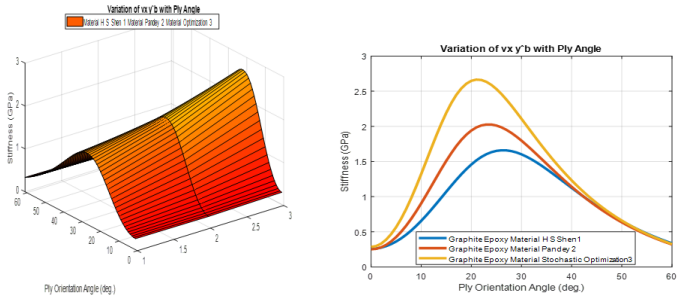

Figure 26 Three types of material properties are analysed for the effects of ply angle 60^{0}on variation of Poisson ratio stiffness (vxy^b).

Figure 27 Three types of material properties are analysed for the effects of ply angle 75^{0}on variation of young modulus stiffness (Ex^b). It is seen that for material 3 properties has higher stiffness magnitude of 275 Gpa where as it is 140 Gpa for material1 properties and has lower value 25 Gpa for material 2 at 0^{0}ply angle and decreases drastically to almost zero for all materials as ply angle increases.

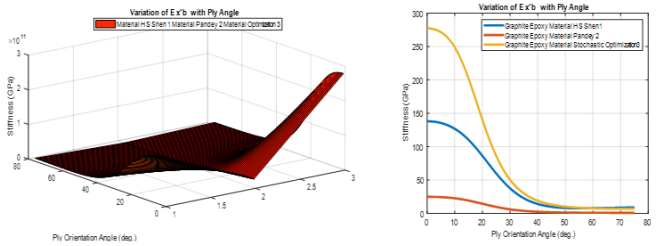

Figure 27 Three types of material properties are analysed for the effects of ply angle 75^{0}on variation of young modulus stiffness (Ex^b).

Figure 28 Three types of material properties are analysed for the effects of ply angle 75^{0}on variation of young modulus stiffness (Ey^b). It is seen that for material 1 properties has higher stiffness magnitude of 9.0 Gpa where as it is 8.0 Gpa for material 3 properties and has lower value 0.2 Gpa for material 2 at 0^{0}ply angle and decreases and increase for material 1 and increases for material 2 and material 3 as ply angle increases.

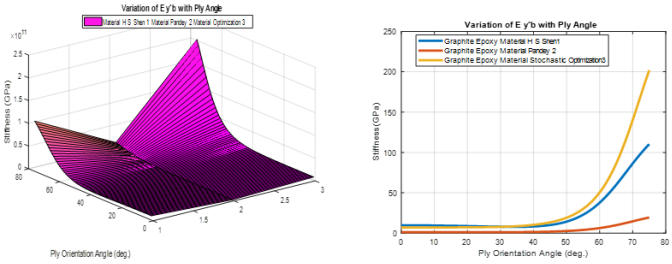

Figure 28 Three types of material properties are analysed for the effects of ply angle 75^{0}on variation of young modulus stiffness (Ey^b).

Figure 29 Three types of material properties are analysed for the effects of ply angle 75^{0}on variation of shear modulus stiffness (Gxy^b). It is seen that for material 3 properties has higher stiffness magnitude of 3.0 GPa where as it is 2.5 GPa for material 1 properties and has lower value 0.1 GPa for material 2 at 0^{0}ply angle and increases and decreases for all materials as ply angle increases.

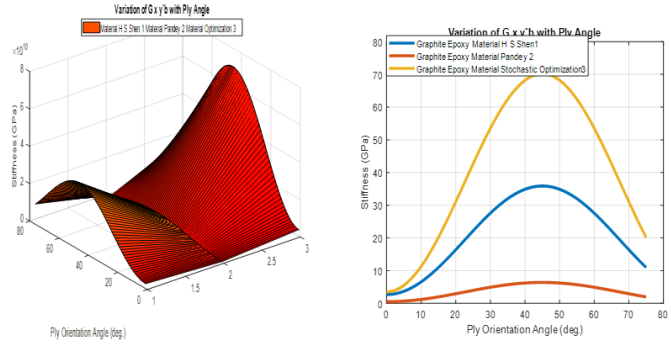

Figure 29 Three types of material properties are analysed for the effects of ply angle 75^{0}on variation of shear modulus stiffness (Gxy^b).

Figure 30 Three types of material properties are analysed for the effects of ply angle 75^{0}on variation of Poisson ratio Poisson ratio stiffness (vxy^b). It is seen that for all material properties has same stiffness magnitude of 2.5 GPa at 0^{0}ply angle and increases and decreases for all materials as ply angle increases.

Citation: Kumar R. Analysis of parameters considered for subsonic wind tunnel and supersonic wind tunnel design with suitability of material properties useful for blades design:A MATLAB simulation investigation. *Aeron Aero Open Access J.* 2025;9(2):106–116. DOI: 10.15406/aaoaj.2025.09.00241

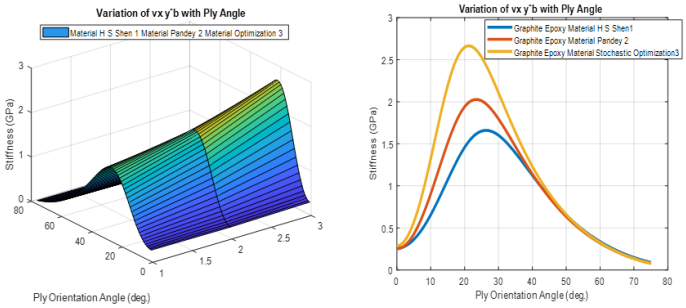

Figure 30 Three types of material properties are analysed for the effects of ply angle 75^{0}on variation of Poisson ratio Poisson ratio stiffness (vxy^b).

Figure 31 Three types of material properties are analysed for the effects of ply angle 90^{0}on variation of young modulus stiffness (Ex^b). It is seen that for material 3 properties has higher stiffness magnitude of 275 Gpa where as it is 140 Gpa for material1 properties and has lower value 25 Gpa for material 2 at 0^{0}ply angle and decreases drastically to almost zero after 60^0 ply angle for all materials as ply angle increases.

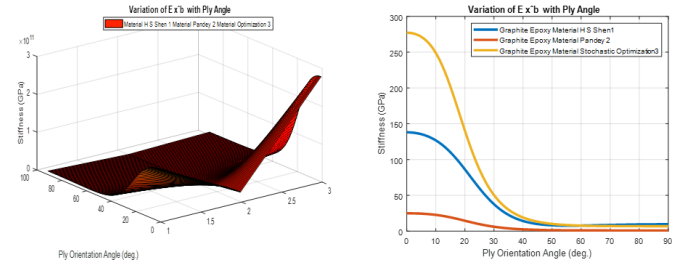

Figure 31 Three types of material properties are analysed for the effects of ply angle 90^{0}on variation of young modulus stiffness (Ex^b).

Figure 32 Three types of material properties are analysed for the effects of ply angle 90^{0}on variation of young modulus stiffness (Ey^b). It is seen that for all materials properties has same stiffness magnitude of 5.0 Gpa at 0^{0}ply angle and decreases up to 40^0 and increase for all materials as ply angle increases.

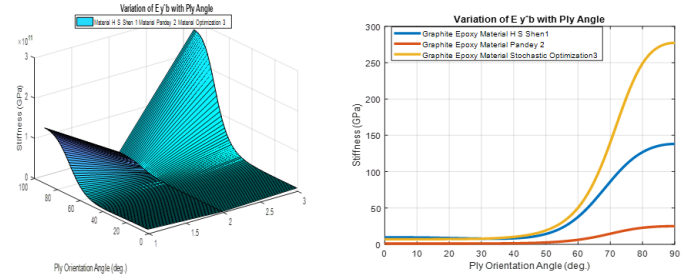

Figure 32 Three types of material properties are analysed for the effects of ply angle 90^{0}on variation of young modulus stiffness (Ey^b).

Figure 33 Three types of material properties are analysed for the effects of ply angle 90^{0}on variation of shear modulus stiffness (Gxy^b). It is seen that for material 3 properties has higher stiffness magnitude of 3.0 GPa where as it is 2.5 GPa for material 1 properties and has lower value 0.1 GPa for material 2 at 0^{0}ply angle and increases and decreases for all materials as ply angle increases.

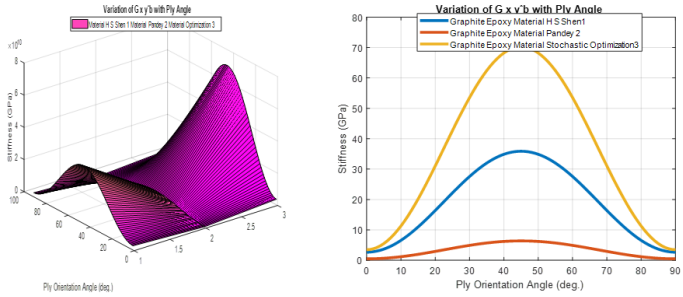

Figure 33 Three types of material properties are analysed for the effects of ply angle 90^{0}on variation of shear modulus stiffness (Gxy^b).

Figure 34 Three types of material properties are analysed for the effects of ply angle 90^{0}on variation of Poisson ratio stiffness (vxy^b). It is seen that for all material properties has same stiffness magnitude of 2.5 GPA at 0^{0}ply angle and increases and decreases for all materials as ply angle increases. It becomes zero finally.

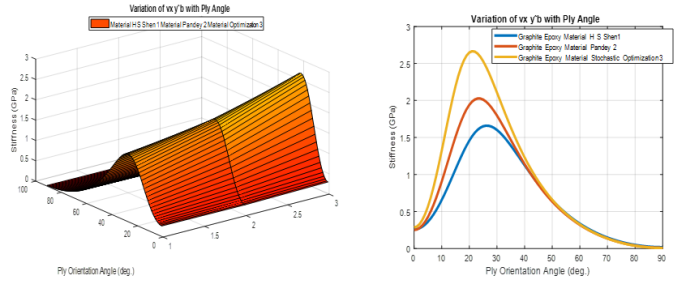

Figure 34 Three types of material properties are analysed for the effects of ply angle 90^{0}on variation of Poisson ratio stiffness (vxy^b).

Results and analysis

On analysis it is seen that for test section the drop of total pressure is higher compared to Nozzle section. Similarly, total pressure drop for diffuser is much higher compared to constant area of wind tunnel. For energy ratio vs volumetric flow rate studied, the losses are less significant. Air mass flow rate significantly increases on increase of throat cross sectional area and also varies on varying stagnation temperature. For small amount of air mass flow rate there is need of higher test duration and then sharp decline occur when the mass flow rate increases and a minimum value reaches.

On varying stagnation temperature of ambient air there is slight variations in test duration curve. Material 3 found to have higher Young modulus stiffness in longitudinal direction, Shear modulus stiffness and Poisson ratio stiffness parameters for ply angles (15^0,30^0,45^0,60^0,75^0 and 90^0) except Young modulus stiffness in lateral direction. However; for ply angle 90^0 the Young modulus stiffness in lateral direction and Poisson ratio stiffness parameters are same for all three kind of material chosen for blade design.

Conclusion

Based on the study carried out for Subsonic and supersonic wind tunnels and blade material choice to be taken in consideration; the following points are concluded. The design of a supersonic wind tunnel for use in the laboratory is focused and various parameters are analysed using MATLAB codes. The salient features are as:

a) Subsonic and supersonic wind tunnels are investigated at test section, nozzle and diffuser at constant area for volumetric flow rate and total pressure drop and energy ratio. Mass flow

Citation: Kumar R. Analysis of parameters considered for subsonic wind tunnel and supersonic wind tunnel design with suitability of material properties useful for blades design:A MATLAB simulation investigation. *Aeron Aero Open Access J.* 2025;9(2):106–116. DOI: 10.15406/aaoaj.2025.09.00241

rate is found out at Throat section area, ratio size of the open to test section, length of tunnel, test section area and stagnation temperature.

b) Mach number and area ratio, test duration and throat height are also investigated. Volumetric flow rate for total pressure drop is significant for test section compared to nozzle, diffuser and constant area.

c) Ratio is influenced by volume flow rate. Mass flow rate is influenced by test duration also. Area ratio makes significant contribution for variations in area ratios and throat height of the tunnel in preset study.

d) Comparing three types material properties, Material 3 found to have higher Young modulus stiffness in longitudinal direction, Shear modulus stiffness and Poisson ratio stiffness parameters for ply angles (15^0,30^0,45^0,60^0,75^0 and 90^0) except Young modulus stiffness in lateral direction. However; for ply angle 90^0 the Young modulus stiffness in lateral direction and Poisson ratio stiffness parameters are same for all three kind of material chosen for blade design

e) The present study can be further extended to practical approach with same input parameters.

Acknowledgement

The author would like to express his sincere appreciation to the anonymous reviewers for their careful analysis, helpful criticism, and insightful ideas that significantly improved this paper. Reviewer's exhaustive review wise comments and attention to detail have greatly enhanced the manuscript's quality and clarity

Data availability: All models or codes generated or used during the study are available from the corresponding author by request. However, the database is proprietary/confidential in nature and may only be provided with restrictions

Conflict of interest

Author has no conflicts of interest.

Funding

No funding is provided by anybody.

References

1. McCabe C. Design of a supersonic nozzle. London, UK: Her Majesty's Stationery Office; 1964.¨b»
2. Barlow JB. Low-speed wind tunnel testing. New York, NY: John Wiley & Sons; 1965.
3. Pope A. High-speed wind tunnel testing. New York, NY: John Wiley & Sons Inc; 1965.
4. Rae AP. Low-speed wind tunnel testing. Seattle, WA: John Wiley & Sons; 1984.
5. Delery J, Marvin J. Shock-wave boundary layer interaction. North Atlantic Treaty Organization, Advisory Group for Aerospace Research and Development; 1986.
6. Sankar L. Observation parts of a wind tunnel. Flights of Inspiration. 1995.
7. Giancoli DC. Physics for scientists and engineers with modern physics. 3rd ed. New Jersey: Prentice Hall; 2000.
8. Anderson J. Research in supersonic flight and the breaking of the sound barrier. *Smithsonian Research Online*. 1998.
9. Anderson JD. Modern compressible flow with historical perspective. New York, NY: McGraw-Hill Higher Education; 2003.
10. Kotwani K. Wind tunnel performance analysis. 2014.
11. Baals D, Corliss W. Wind tunnels of NASA. NASA History Office; 1981.
12. John JE, Keith TG. Gas dynamics. 3rd ed. Upper Saddle River, NJ: Pearson Prentice Hall; 2006.
13. Henry J, Dick S, Garber S. Orders of magnitude: A history of the NACA and NASA. 2007.
14. Carlone G. Building a wind tunnel. 2013.
15. Nott CR, Olcmen SM, Lewis DR, et al. Supersonic, variable-throat, blow-down wind tunnel control using genetic algorithms, neural networks, and gain-scheduled PID. *Appl Intell*. 2008,29:79–89.
16. Lu FK, Matsumoto J, Wilson DR. Rapid valve opening technique for supersonic blow-down tunnel. *Exp Therm Fluid Sci*. 2009,33(3):551–554.
17. Baals DD. Whirling arms and the first wind tunnels. *NASA*. 2009.
18. Aerolab, Aerolab, Anderson JD. Modern compressible flow. New York: McGraw-Hill. 2013
19. Harris TA, Carl WJ. The Vertical Wind Tunnel of the National Advisory Committee for Aeronautics. *NASA*. 2013.
20. Barlow JB, Rae WH, Pope A. Low-speed wind tunnel testing. 3rd ed. New York, NY: John Wiley & Sons; 1999.
21. Williams RB. Nonlinear mechanical and actuation characterization of piezoceramic fiber composites. PhD thesis. Virginia Polytechnic Institute and State University; 1999.
22. Kudva J. Overview of the DARPA smart wing project. *J Intell Mater Syst Struct*. 2004;15(4):261–267.
23. Vos R, Breuker RD, Barrett R, et al. Morphing wing flight control via postbuckled precompressed piezoelectric actuators. *J Aircraft*. 2007;44(4):1060.
24. Bilgen O. Macro fiber composite actuated unmanned air vehicles: design, development, and testing. Master's thesis. Virginia Polytechnic Institute and State University; 2007.
25. Flanagan JS, Strutzenberg RC, Myers RB, et al. Development and flight testing of a morphing aircraft: the NextGen MFX-1. In: Proceedings of the AIAA/ASME/ASCE/AHS/ASC Structures, Structural Dynamics, and Materials Conference; 2007.
26. Stewart K, Wagener J, Abate G, et al. Design of the Air Force Research Laboratory micro aerial vehicle configurations. In: Proceedings of the AIAA Conference; 2007.
27. Barbero EJ. Finite element analysis of composite materials. Boca Raton, FL: CRC Press; 2007.
28. Bilgen O, Kochersberger KB, Inman DJ, et al. Lightweight high-voltage electronic circuits for piezoelectric composite actuators. *J Intell Mater Syst Struct*. 2010;21(14):1417–1426.
29. Bilgen O. Aerodynamic and electromechanical design, modeling, and implementation of piezocomposite airfoils. PhD thesis. Virginia Polytechnic Institute and State University; 2010.
30. Smart Material Corporation. Smart materials catalog. Published May 2011.
31. Shen HS. Hygrothermal effects on the postbuckling of shear-deformable laminated plates. *Int J Mech Sci*. 2001;43(5):1259–1281.
32. Pandey R. Hygrothermoelastic postbuckling response of laminated composite plates. *J Aerosp Eng*. 2010;23(1).
33. Aydin L, Artem HS. Comparison of stochastic search optimization algorithms for laminated composites under mechanical and hygrothermal loadings. *J Reinf Plast Compos*. 2011;30(4):1197–1212.